Biochemical Pharmacology 84 (2012) 292–302

Contents lists available at SciVerse ScienceDirect

Biochemical Pharmacology

journal homepage: www.elsevier.com/locate/biochempharm

Uncoupling of K^+ and Cl^- transport across the cell membrane in the process of regulatory volume decrease

Linjie Yang [a], Linyan Zhu [a], Yue Xu [b], Haifeng Zhang [c], Wencai Ye [d], Jianwen Mao [e], Lixin Chen [a,*], Liwei Wang [c,*]

[a] Department of Pharmacology, Medical College, Jinan University, Guangzhou 510632, China
[b] Xuyue (Beijing) Science & Technology Co., Ltd., Beijing 100080, China
[c] Department of Physiology, Medical College, Jinan University, Guangzhou 510632, China
[d] College of Pharmacy, Jinan University, Guangzhou 510632, China
[e] Guangdong Key Laboratory for Bioactive Drugs Research and, Guangdong Pharmaceutical University, Guangzhou 510006, China

ARTICLE INFO

Article history:
Received 20 March 2012
Received in revised form 5 May 2012
Accepted 7 May 2012
Available online 14 May 2012

Keywords:
Ion-selective electrode
Patch-clamp technique
Ion transport
Cell size
Tumor cell

ABSTRACT

It is accepted that K^+ and Cl^- flows are coupled tightly in regulatory volume decrease (RVD). However, using self referencing microelectrodes, we proved that K^+ and Cl^- transport mainly by channels in RVD was uncoupled in nasopharyngeal carcinoma CNE-2Z cells, with the transient K^+ efflux activated earlier and sustained Cl^- efflux activated later. Hypotonic challenges decreased intracellular pH (pH_i), and activated a proton pump-dependent H^+ efflux, resulting in a decline of extracellular pH (pH_o). Modest decreases of pH_o inhibited the volume-activated K^+ outflow and RVD, but not the Cl^- outflow, while inhibition of H^+ efflux or increase of pH_o buffer ability promoted K^+ efflux and RVD. The results suggest that the temporal dynamics of K^+ channel activities is different from that of Cl^- channels in RVD, due to differential sensitivity of K^+ and Cl^- channels to pH_o. H^+ efflux may play important roles in cell volume regulation, and may be a therapeutic target for human nasopharyngeal carcinoma.

1. Introduction

Cell volume regulation is fundamental for various cell functions [1–4]. Cell proliferation requires an increase of cell volume before cell division [5]. Apoptosis is normally accompanied by cell shrinkage [6]. Cell migration needs precise regulation of cell volume to guarantee correct polarity and hence direction of movement [7]. Cell volume regulation in these processes requires the participation of ion transport across the cell membrane through various transporters and ion channels [8–10]. Volume-activated K^+ and Cl^- channels play important roles in regulatory volume decrease (RVD) induced by cell swelling and in cell volume maintenance under normal osmotic conditions, as well as in various cell functions [1–4,11–15]. The activation and the pharmacological properties of volume-activated K^+ and Cl^- channels have been widely studied using patch clamp techniques. However the activation and activities of the channels under non-invasive conditions have not been clarified because of the limitation of patch clamp techniques.

With patch clamp techniques, channels are always isolated, or the cell content is disturbed. For instance, a global acidification in RVD has been identified [16,17] and hypotonic stimulation can induce a decrease of intracellular pH even as large as 0.7 pH units. The changes of pH may affect the activities of ion channels [18–21]. However, in the experiments performed with the whole-cell patch clamp technique, the intracellular pH is restricted to the pH of pipette solution, and the dynamic changes of intracellular pH in RVD are normally prevented. In cell-attached single channel recordings, the extracellular environment of channels is isolated and restricted. The dynamic changes of ion channel activities or ion flows under undisturbed physiological conditions are thus difficult to be recorded using patch clamp techniques and a non-invasive technique is needed to solve these problems.

The non-invasive micro-test technique is a technique capable of studying the ion movements of cells without mechanical contact between the recorded cell and the electrode using self-referencing ion-selective microelectrodes [22–24]. It is able to "micro-sample" ion activities and measure diffusion gradient and ion fluxes even in single cells [22–24]. The ion-selective microelectrodes can also pose a barrier to simple diffusion, creating an ion trap close to the plasma membrane. The technique provides the advantage of amplifying the local change in ion concentration without

* Corresponding authors. Tel.: +86 20 85220260; fax: +86 20 85221343.
E-mail addresses: eyanglinjie@163.com (L. Yang), yandeer@yahoo.com.cn (L. Zhu), wongkinglw@hotmail.com (Y. Xu), zhanghaifeng19840305@yahoo.com.cn (H. Zhang), wangchenlixin@hotmail.com (W. Ye), jianwenmao@hotmail.com (J. Mao), chenlixinw@sohu.com (L. Chen), wangliweic@sohu.com (L. Wang).

0006-2952/$ – see front matter © 2012 Published by Elsevier Inc.
http://dx.doi.org/10.1016/j.bcp.2012.05.006

dramatically changing the rise or fall time of the ion profile, which other ion-mapping techniques do not possess [25]. These advantages ensure it to be an ideal technique for measurements of ion transport in living cells without interfering cellular content or regulation mechanisms. The technique is also capable of measuring the extracellular pH close to the cell membrane.

In this study, the temporal dynamics of the transmembrane transport of K^+, Cl^- and H^+ in the process of hypotonicity-induced RVD were first investigated using the non-invasive micro-test technique in intact human nasopharyngeal carcinoma CNE-2Z cells. The measurements of ion effluxes revealed a differential time course of different ions, which may be associated with the secretion of H^+ and the different sensitivities of various ion channels to the changes of pH.

2. Materials and methods

2.1. Cell preparation

The poorly differentiated human nasopharyngeal carcinoma CNE-2Z cells were routinely grown in 25 cm^2 plastic tissue culture flasks in the RPMI 1640 medium containing 10% fetal calf serum, 100 IU/ml penicillin and 100 μg/ml streptomycin, and incubated in a humidified atmosphere of 5% CO_2 at 37 °C. The cells were subcultured every 2 days. For ion flux and current measurements, cells that had been cultured for 48 h and reached 80% confluency were trypsinized, centrifuged and re-suspended in the culture medium. Cell suspension was plated on round coverslips of 22 mm in diameter (150 μl/coverslip), which were located in 35 mm tissue culture dishes, and was then incubated at 37 °C for 2–3 h before the measurements of ion flux, current or cell volume.

2.2. Preparation of ion-selective electrodes

Ion-selective electrodes were prepared according to the protocols described by Smith and Trimarchi [23]. Microelectrodes with a tip diameter of 2–4 μm were pulled from borosilicate glass capillaries on a two-stage vertical puller. The microelectrodes were oven dried at 180 °C for 3 h and treated at 180 °C for 1 h in a beaker containing silanizing compound vapor, which was achieved by adding 100 μl silanizing compound tributylchlorosilane (Sigma Aldrich, St. Louis, MO, USA) in the beaker. Dried and cooled electrodes were back filled with the back-filled solutions (15 mM NaCl plus 40 mM KH_2PO_4 for H^+ flux measurements, 100 mM KCl for K^+ and Cl^- flux measurements), and the electrode tips were front filled with the commercially available ionophore cocktails, the liquid ion exchangers (LIX; Fluca, Sigma Aldrich, St. Louis, MO, USA). The prepared electrode was inserted into a half-cell microelectrode holder (XYEH01-1, Younger USA Sci. & Tech. Co., Applicable Electronics Inc. and Science Wares Inc, USA) equipped with a silver chloride-coated silver wire.

The Nernstian properties of each electrode were measured by placing the electrode in a series of standard calibration solutions based on the extracellular solutions for ion flux measurements. The electrodes were calibrated in standard solutions before and after use, and only the electrodes possessing Nernst slopes were used.

2.3. Non-invasive ion flux measurements

Measurements of net Cl^-, K^+, and H^+ fluxes were performed using the non-invasive micro-test technique described previously [24] with a recording system (BIO-001A, Younger USA Sci. & Tech. Co., Applicable Electronics Inc. and Science Wares Inc, USA). Measurements of ion flux of single cells rely on the establishment of an ion gradient generated on the cell surface. The ion-selective electrode was controlled to move between two poles, the far and near poles (with the near pole 1–2 μm away from the cell surface), with an excursion of 10 μm at a programmable frequency of 0.3 Hz. Voltages at each pole, representing the Nernst potential of the solution and the ion activity at each point, were measured. In the presence of a flux, the voltages varied between the two poles. The recorded potential differences were converted into electrochemical potential differences using the calibrated Nernst slopes of the electrodes. Data and image acquisition, preliminary processing and control of the three-dimensional electrode positioner were performed with the system-equipped ASET software. The system sampled at 1 kHz, and approximately one third of the data during and after each movement were discarded to account for gradient disturbance and system response time. Signals at each position were averaged and the signal of the far pole was subtracted from that of the near pole.

For Cl^- flux measurements, the isotonic extracellular solution contained (in mM): 70 NaCl, 0.5 $MgCl_2$, 2 $CaCl_2$, 1 HEPES, 2 KCl, and 147.5 D-mannitol. The concentration of KCl in the solution was reduced to 0.5 mM for K^+ flux measurements, while 0.15 mM KH_2PO_4 and 0.8 mM Na_2HPO_4 were used to substitute HEPES for H^+ flux measurements. The osmolarity of the solutions was measured with a freezing-point osmometer (OSMOMAT 030; Gonotec, Germany). The osmolarity of isotonic solutions was adjusted to 300 mOsmol/l with D-mannitol. The hypotonic solutions were obtained by omitting the D-mannitol from the isotonic solutions, giving an osmolarity of 160 mOsmol/l (47% hypotonicity, compared to the isotonic solution). The pH of the extracellular solutions was adjusted to 7.40 with NaOH.

We have reported that the Cl^- channel blockers 5-nitro-2-(3-phenylpropylamino) benzoic acid (NPPB) and tamoxifen can inhibit the hypotonicity-activated Cl^- currents and RVD in CNE-2Z cells [1]. However, it has been reported that NPPB (50 μM) but not tamoxifen (10 μM) can destroy the Nernstian characteristics of the Cl^- selective electrode [26]. We chose tamoxifen as the Cl^- channel blocker. The addition of the potassium channel blocker clotrimazole (CLT, 100 μM) or the proton pump inhibitor omeprazole (20 μM), which has been reported to be able to inhibit the H^+ secretion via proton pump [27], to standard calibration solutions had little effects on the Nernstian slope of K^+ or H^+ selective electrodes. Clotrimazole was dissolved with DMSO in the concentration of 40 mM. Tamoxifen and omeprazole were dissolved with methanol in the concentrations of 10 mM and 50 mM, respectively. They were diluted to the indicated final concentrations using corresponding solutions for different experiments. All chemicals were purchased from Sigma Aldrich (St. Louis, MO, USA).

Cells were first exposed to isotonic extracellular solution for 20 min before experiments. The ion selective electrode was posited vertically 500 μm above the cell for 3–5 min to record the background signal (Blank), and placed 1–2 μm from the cell membrane for 3–5 min to record the isotonic control signal (Iso). The isotonic bath solution was then exchanged 3 times with the hypotonic bath solution.

2.4. Patch clamp electrophysiology

Whole-cell currents of single CNE-2Z cells were recorded using the patch-clamp technique previously described [28], with a List EPC-7 patch-clamp amplifier (List Electronic, Darmstadt, Germany). For whole-cell Cl^- current recordings, the pipette solution contained (in mM): 70 N-methyl-D-glucamine chloride (NMDG-Cl), 1.2 $MgCl_2$, 10 HEPES, 1 EGTA, 140 D-mannitol and 2 ATP, and the isotonic bath solution contained: 70 NaCl, 0.5 $MgCl_2$, 2 $CaCl_2$, 10 HEPES, and 140 D-mannitol. For whole-cell K^+ current recordings, the pipette solution contained: 134 K-Gluconate, 10 KCl, 1 $MgCl_2$, 0.08 $CaCl_2$, 0.03 EGTA, 10 HEPES, and 2 Na_2ATP. The

isotonic bath solution contained: 66 Na-Gluconate, 1 $MgSO_4$, 2 NaCl, 4 K-Gluconate, 2 $CaSO_4$, 10 HEPES, and 140 D-mannitol. The osmolarity of the pipette and isotonic solutions was adjusted to 300 mOsmol/L with D-mannitol. The 47% hypotonic bath solutions were obtained by omitting the D-mannitol from the isotonic solutions. The pH of the pipette and bath solutions was adjusted to 7.25 and 7.40 with Tris-base, respectively. Experiments were carried out at room temperature (20–24 °C).

The patch clamp pipettes were made from standard wall borosilicate glass capillaries and gave a resistance of 5–10 MΩ when filled with pipette solutions. Cell capacitance compensation and series resistance compensation were used to minimize voltage errors. The amplifier reading of capacitance was used as the value for whole-cell membrane capacitance. Once the whole-cell configuration was established, cells were held at 0 mV and then stepped repeatedly to 200 ms pulses of 0, ±40 and ±80 mV for Cl^- current recordings and 0, ±46 and ±92 mV for K^+ current recordings, with 4 s intervals between steps. Command voltages and whole-cell currents were recorded simultaneously on a computer via a laboratory interface (CED 1401, Cambridge, UK) with a sampling rate of 3 kHz. The voltage pulse generation, data collection and current analysis were performed using EPC software (CED, Cambridge, UK).

In analysis of data collected, all current measurements were made at 10 ms after onset of each voltage step. The inhibition of volume-activated Cl^- and K^+ currents were calculated using the following equation: $(Current_{Hypo} - Current_{Inhib})/(Current_{Hypo} - Current_{Iso}) \times 100\%$, where $Current_{Hypo}$ is the peak current recorded under hypotonic stimulation, $Current_{Inhib}$ is the current recorded after inhibitory treatments, and $Current_{Iso}$ is the current recorded under isotonic conditions.

2.5. Extracellular and intracellular pH measurements

Extracellular pH near the cell surface was detected using the H^+ selective electrodes. The pH was computed from the voltage measured 1–2 μm from the cell membrane, which represents the H^+ activity of the extracellular micro-environment. Intracellular pH was measured using the dual-excitation ratio method with the pH sensitive dye 2′,7′-Bis-(2-carboxyethyl)-5- (and-6)-carboxyfluorescein acetoxymethyl ester (BCECF-AM; Beyotime Institute of Biotechnology, Jiangsu, China) [29]. The isotonic and hypotonic bath solutions for intracellular pH measurements were the same with the bath solutions for whole-cell Cl^- current recordings. The pH of the bath solution for intracellular pH measurements was adjusted to 7.40 with NaOH. Employing a digital fluorescence microscopy system, pH sensitive dye was excited at 460 and 488 nm and the fluorescence emitted at 520 nm was detected in turn. Analysis was restricted to the cells able to retain the fluorescent indicator. Raw intensity data at each excitation wavelength were corrected for background fluorescence prior to calculation of the ratio. The ratios of background-corrected emission intensities (I_{488}/I_{460}) were transformed into intracellular pH.

2.6. Volume measurements

Cell images were recorded simultaneously with ion flux measurements, and the volume change of the cell was estimated from the cell image. Cell images were captured by a charge-coupled device digital camera (Mono CCD625, Leica, Germany) which was connected to the microscope (Leitz DMIL; Leica Mikroskopie und

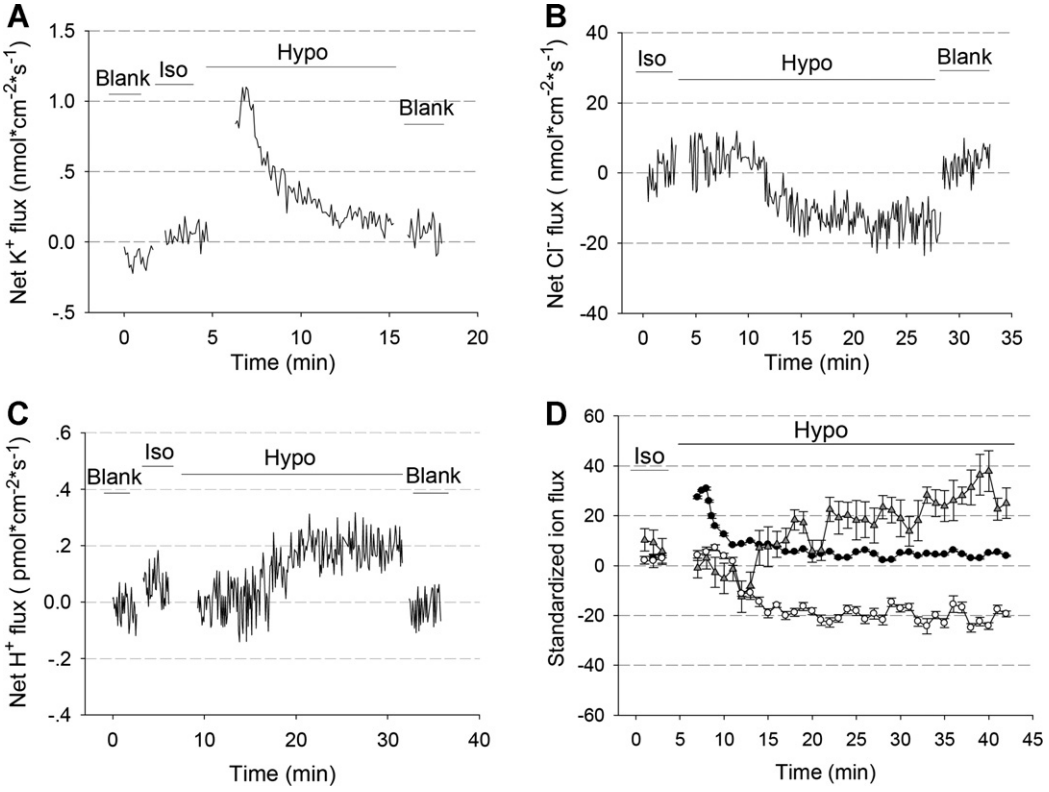

Fig. 1. Dynamic K^+, Cl^- and H^+ fluxes across the cell membrane induced by 47% hypotonic challenges in CNE-2Z cells. (A) The typical time-course of K^+ fluxes activated by 47% hypotonic solution and recorded by the non-invasive micro-test technique. The Cell was exposed to the isotonic solution (Iso) for several minutes to establish a baseline flux, and then the bath solution was exchanged with 47% hypotonic solution (Hypo) as indicated. Background (Blank) flux was measured by moving the electrode 500 μm away from the cell. The upward deflection of the signal indicates K^+ efflux from the cell. (B) The typical time-course of Cl^- fluxes activated by 47% hypotonic solution and recorded by the non-invasive micro-test technique. The downward deflection of the signal indicates Cl^- efflux. (C) The typical time-course of H^+ fluxes activated by 47% hypotonic solution and recorded by the non-invasive micro-test technique. The upward deflection of the signal indicates H^+ efflux. (D) Comparison of K^+, H^+, and Cl^- effluxes (n = 11–14 cells for different ion flux recording, mean ± S.E.M).

Systeme, Germany). The acquisition of the cell images was controlled by the Quantimet Q500MC image processor and analysis software (Leica, Germany). Cell volume was calculated with the equation $V = 4/3 \times S \times (S/\pi)^{1/2}$, where S is the area (μm^2) [30]. Cell volume was standardized by dividing the cell volume in treatments with the control cell volume in isotonic solutions.

2.7. Statistical analysis

Data were expressed as means ± S.E.M. (number of observations) and, where appropriate, were analyzed using ANOVA (SPSS version 11.5; Chicago, IL, USA). Statistical significance was defined as $P < 0.05$ or 0.01. All experiments were repeated at least 5 times.

3. Results

3.1. Differential temporal dynamics of hypotonicity-induced K^+, Cl^- and H^+ fluxes

The transmembrane K^+, Cl^- and H^+ fluxes in single CNE-2Z cells under 47% hypotonic condition were recorded using the non-invasive micro-test technique. The results showed that exposure of cells to 47% hypotonic solution induced effluxes of K^+, Cl^- and H^+ (Fig. 1). However, the time-courses of K^+, Cl^- and H^+ effluxes were different.

The activation of K^+ efflux induced by hypotonic stimulation was ahead of Cl^- efflux. The K^+ efflux peaked within 2 min and then declined gradually in all the cells observed (Fig. 1A). Opposite to the fast activation of K^+ efflux, the activation of Cl^- efflux was much slower, with a latency of about 5 min. Once activated, the Cl^- efflux was maintained in a relative high level when the cells were still bathed in the hypotonic solution in the periods observed (25–60 min, Fig. 1B).

Similar to that of Cl^- efflux, the activation of H^+ efflux induced by hypotonic stimulation was slow. The H^+ efflux was not decreased in the time period observed. H^+ effluxes remained at a relative high level for more than 20 min (Fig. 1C). The comparisons of different ion flows were shown in Fig. 1D. The results indicated that hypotonic challenges induced a transient K^+ efflux which was followed by sustained Cl^- and H^+ efflux.

3.2. Inhibition of K^+ efflux by potassium channel blockers

The hypotonicity-induced K^+ efflux could be abolished almost completely by the Ca^{2+}-activated intermediate conductance K^+ channel (IK channel) blocker clotrimazole (100 μM, Fig. 2A). Mean K^+ efflux was reduced from 0.63 ± 0.15 nmol cm^{-2} s^{-1} ($n = 11$) to 0.06 ± 0.14 nmol cm^{-2} s^{-1} ($n = 6$, $P < 0.05$) (Fig. 2B). The results suggest that the hypotonicity-induced K^+ efflux is mainly mediated by Ca^{2+}-activated intermediate conductance K^+ channels.

Patch-clamp experiments demonstrated that only a weak background K^+ current was recorded in the isotonic bath solution, and exposure of cells to 47% hypotonic solution activated a K^+ current in about 1–2 min (Fig. 2C). The current was inhibited by the K^+ channel blocker clotrimazole (100 μM) by 88.13 ± 7.86% at −92 mV and 92.97 ± 4.97% at +92 mV ($n = 5$, $P < 0.01$) (Fig. 2D).

The K^+ current recorded with the patch clamp technique was different from the K^+ efflux detected by the non-invasive

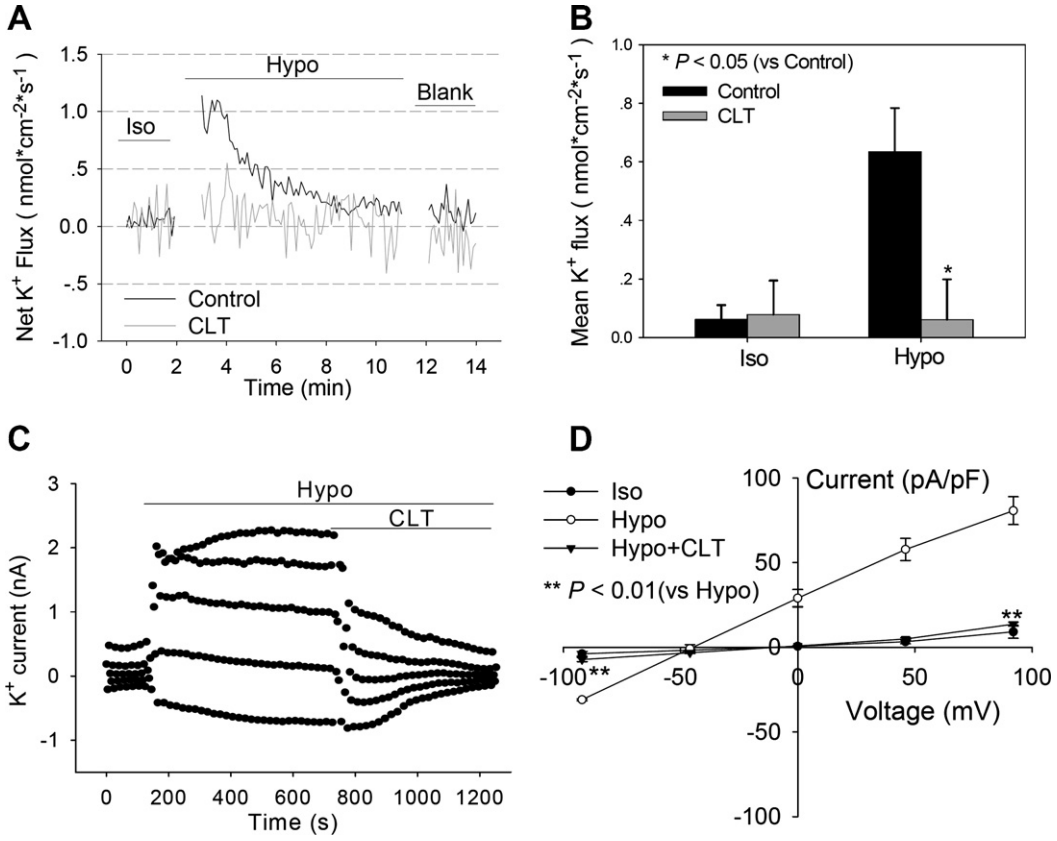

Fig. 2. Inhibition of hypotonicity-induced K^+ efflux and K^+ current by the potassium channel blocker clotrimazole (CLT). (A) The time-course of K^+ efflux induced by hypotonic stimulation and inhibition of the K^+ efflux by 100 μM clotrimazole, detected by the non-invasive micro-test technique. Iso, isotonic bath solution. Hypo, 47% hypotonic solution. Blank, ion flux measured by moving the electrode 500 μm away from cells. (B) Mean K^+ effluxes measured under different conditions ($n = 11$ cells for Control, $n = 6$ cells for CLT, mean ± S.E.M. $^*P < 0.05$, t-test, compared with Control). (C) The time-course of K^+ current induced by hypotonic stimulation and inhibition of the current by 100 μM clotrimazole, recorded with the patch clamp technique. Cells were held at 0 mV and then stepped repeatedly to 0, ±46 and ±92 mV with 4 s intervals between steps. (D) Mean K^+ currents under different conditions ($n = 5$ cells, mean ± S.E.M., $^*P < 0.05$, $^{**}P < 0.01$, Paired t-test, compared with Hypo).

micro-test technique. The hypotonicity-induced K^+ efflux declined gradually in a few minutes (Fig. 2A), but no significant decline was observed in the hypotonicity-activated K^+ current (Fig. 2C).

3.3. Inhibition of Cl^- efflux by chloride channel blockers

The chloride channel blocker tamoxifen could inhibit the hypotonicity-activated Cl^- efflux (Fig. 3A). Mean Cl^- efflux was reduced from -9.66 ± 2.66 nmol cm^{-2} s^{-1} ($n = 9$) to -0.94 ± 2.27 nmol cm^{-2} s^{-1} ($n = 6$, $P < 0.05$) by 10 μM tamoxifen (Fig. 3B), indicating that the Cl^- efflux is mainly carried by volume-sensitive chloride channels.

A tamoxifen-sensitive Cl^- current was also recorded using the whole-cell patch-clamp technique when cells were exposed to 47% hypotonic solution (Fig. 3C). The current was activated in 1–2 min and reached the peak in 3–5 min. Tamoxifen (10 μM) inhibited almost completely the current (Fig. 3C and D).

Further analysis of the Cl^- efflux detected by the non-invasive micro-test technique and the Cl^- current recorded with the patch clamp technique indicated that the activation process was similar. Once activated by the hypotonic challenges, both the Cl^- efflux and current were sustained, with no inactivation observed. However, the activation latency of Cl^- efflux was longer (about 5 min) than that of Cl^- current.

3.4. Inhibition of H^+ efflux by omeprazole and extracellular calcium depletion

The baseline of H^+ flux (Blank) was recorded 500 μm above the cells. When the recording electrode was positioned 1–2 μm away from the cell, a weak H^+ efflux was detected under isotonic conditions (Iso). The H^+ efflux elevated significantly 5–8 min after the isotonic bath solution was replaced with 47% hypotonic bath solution (Hypo). The hypotonicity-activated H^+ efflux was inhibited by the H^+ pump inhibitor omeprazole (20 μM) (Fig. 4A). The H^+ efflux was decreased from 0.27 ± 0.05 pmol cm^{-2} s^{-1} to 0.12 ± 0.03 pmol cm^{-2} s^{-1} ($n = 5$, $P < 0.01$).

The activation of hypotonicity-induced H^+ efflux could be prevented by depletion of extracellular calcium (Fig. 4B and C). Exposure of cells to the Ca^{2+}-free hypotonic solution did not induced significantly H^+ efflux. The H^+ efflux in the Ca^{2+}-free hypotonic solution was 0.04 ± 0.03 pmol cm^{-2} s^{-1} ($n = 5$), which was much smaller than that (0.27 ± 0.05 pmol cm^{-2} s^{-1}, $n = 5$, $P < 0.01$) recorded in the control hypotonic solution.

3.5. Changes of extracellular and intracellular pH induced by hypotonic stimulation

The extracellular pH at the position of 1–2 μm away from the cell membrane was detected using the non-invasive micro-test technique. The pH measured 500 μm above cells was taken as the background recording (Blank). In the isotonic bath solution, the extracellular pH recorded 1–2 μm away from the cells was 7.37 ± 0.02, which was a little lower than the Blank (7.39 ± 0.03, $n = 5$, $P < 0.05$). When the cells were challenged with 47% hypotonic solution, the extracellular pH decreased gradually in 5–8 min (7.19 ± 0.03, $n = 5$, $P < 0.01$) and reached a stable level in 15 min (Fig. 5A). The hypotonicity-induced decrease of extracellular pH was inhibited significantly by the proton pump inhibitor omeprazole (20 μM), and the extracellular pH under isotonic conditions was

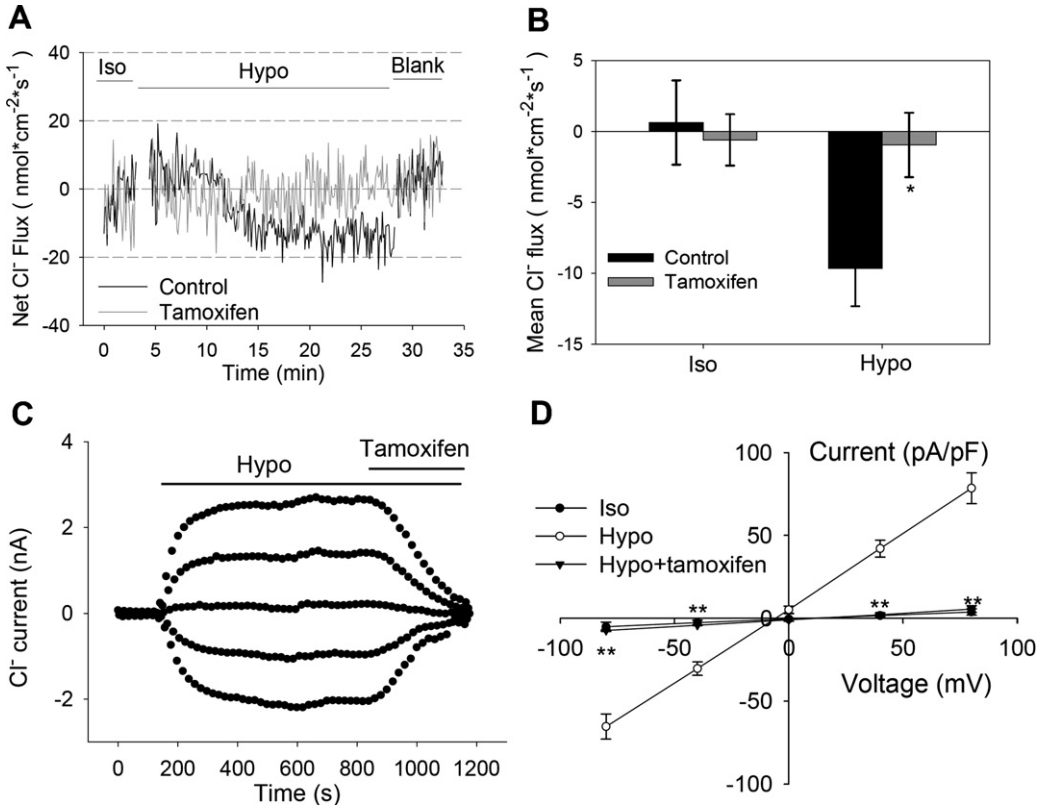

Fig. 3. Inhibition of hypotonicity-induced Cl^- efflux and Cl^- current by the chloride channel blocker tamoxifen. (A) The typical time-course of Cl^- efflux induced by hypotonic stimulation and inhibition of the Cl^- efflux by 10 μM tamoxifen, detected by the non-invasive micro-test technique. Iso, isotonic bath solution. Hypo, 47% hypotonic solution. Blank, ion flux measured by moving the electrode 500 μm away from cells. (B) Mean Cl^- effluxes measured under different conditions ($n = 12$ cells for Control, $n = 6$ cells for tamoxifen, mean ± S.E.M., $^*P < 0.05$, t-test, compared with Control). (C) The typical time-course of Cl^- current induced by hypotonic stimulation and inhibition of the current by 10 μM tamoxifen, recorded with the patch clamp technique. Cells were held at 0 mV and then stepped repeatedly to 0, ±40 and ±80 mV with 4 s intervals between steps. (D) Mean Cl^- currents under different conditions ($n = 5$ cells, mean ± S.E.M., $^{**}P < 0.01$, Paired t-test, compared with Hypo).

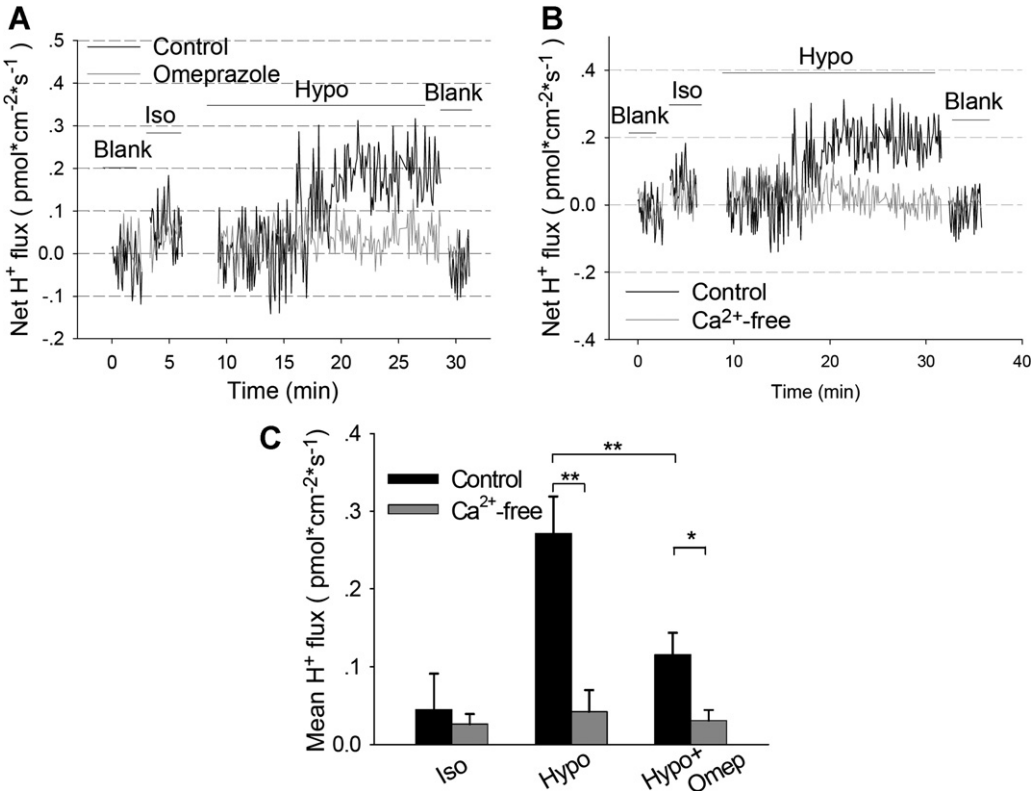

Fig. 4. Inhibition of hypotonicity-induced H^+ efflux by the H^+ pump inhibitor omeprazole (Omep) and extracellular calcium depletion. (A) The time-course of H^+ efflux in response to the hypotonic challenge (Control) and inhibition of H^+ efflux by 20 μM omeprazole, detected by the non-invasive micro-test technique. Iso, isotonic bath solution. Hypo, 47% hypotonic solution. Blank, ion flux measured by moving the electrode 500 μm away from cells. (B) The time-course of H^+ efflux induced by hypotonic bath solution (Control) and the response to the hypotonic stimulation caused by the Ca^{2+}-free hypotonic bath solution containing 2 mM EGTA (Ca^{2+}-free). (C) Mean H^+ effluxes under different conditions ($n = 5$ cells for each groups, mean ± S.E.M., $^*P < 0.05$, $^{**}P < 0.01$, *t*-test).

increased from 7.37 ± 0.02 ($n = 5$) to 7.39 ± 0.01 ($n = 10$, $P < 0.01$) by the omeprazole treatment (Fig. 5A).

The intracellular pH of single CNE-2Z cells was detected using the pH sensitive fluorescent dye BCECF. Similar to the changes of extracellular pH, intracellular pH was also decreased from 7.19 ± 0.02 to 6.68 ± 0.04 by the hypotonic challenge ($n = 5$, $P < 0.01$) (Fig. 5B). However, the time courses of changes were different between the intracellular and extracellular pH. The decrease of intracellular pH was ahead of the drop of extracellular pH (Fig. 5C). Significant decrease of intracellular pH was observed in 1–2 min and peaked in 4–5 min, while the decline of extracellular pH appeared in 5–8 min and reached a stable level in 15 min. The intracellular pH was recovered gradually once the hypotonic effect reached the peak. Further analysis indicated that the time course of hypotonicity-induced K^+ efflux was similar to the change of extracellular pH (Fig. 5C), implying a relationship between K^+ efflux and extracellular pH.

3.6. Inhibition of K^+ transport by extracellular acidity

Further experiments indicate that extracellular pH can modulate the hypotonicity-induced K^+ efflux. As shown in Fig. 6A and B, the K^+ efflux activated by hypotonic solutions at pH 6.5 was much smaller, compared with that at pH 7.4. The K^+ efflux was reduced from 1.00 ± 0.20 nmol cm^{-2} s^{-1} at pH 7.4 ($n = 11$) to 0.22 ± 0.07 nmol cm^{-2} s^{-1} at pH 6.5 ($n = 6$, $P < 0.05$). The results indicate that hypotonicity-induced K^+ efflux is pH-sensitive; Extracellar acidity inhibits K^+ transport across the cell membrane.

The inhibitory effect of extracellular acidity on K^+ transport was further confirmed using the patch clamp technique (Fig. 6C and D). The hypotonicity-activated K^+ current was decreased by 59.64 ± 9.46% at +92 mV and 48.34 ± 15.32% at −92 mV when extracellular pH was decreased from 7.4 to 6.5 ($n = 6$, $P < 0.05$).

3.7. Facilitation of hypotonicity-induced K^+ efflux by inhibition of H^+ secretion and by increase of pH buffer ability

The above results showed that hypotonic stimulation activated H^+ secretion. To investigate the role of hypotonicity-activated H^+ secretion in regulation of K^+ transport, the proton pump inhibitor omeprazole and HEPES were used to block H^+ secretion and to buffer the activity of secreted H^+, respectively. Extracellular application of 20 μM omeprazole increased slightly the extracellular pH (Fig. 5A) and the background K^+ efflux under the isotonic condition, and enhanced the K^+ efflux induced by hypotonic stimulation (Fig. 6E). The hypotonicity-induced K^+ efflux was increased by 38.5% by omeprazole in 4 min ($n = 10$–12 cells for different conditions).

The background and hypotonicity-induced K^+ effluxes were also facilitated by increasing extracellular pH buffer ability (Fig. 6F and G). Increasing the concentration of the pH buffer HEPES to 10 mM from 1 mM enhanced the hypotonicity-induced K^+ efflux by about 37.6% in 4 min ($n = 10$–12 cells for different conditions).

3.8. Regulation of Cl^- transport by extracellular pH

The effects of extracellular pH on hypotonicity-induced Cl^- efflux and current were different from those on hypotonicity-induced K^+ efflux and current. The decrease of extracellular pH to 6.5 from 7.4 did not inhibited, but facilitated the activation of hypotonicity-induced Cl^- efflux and Cl^- current (Fig. 7).

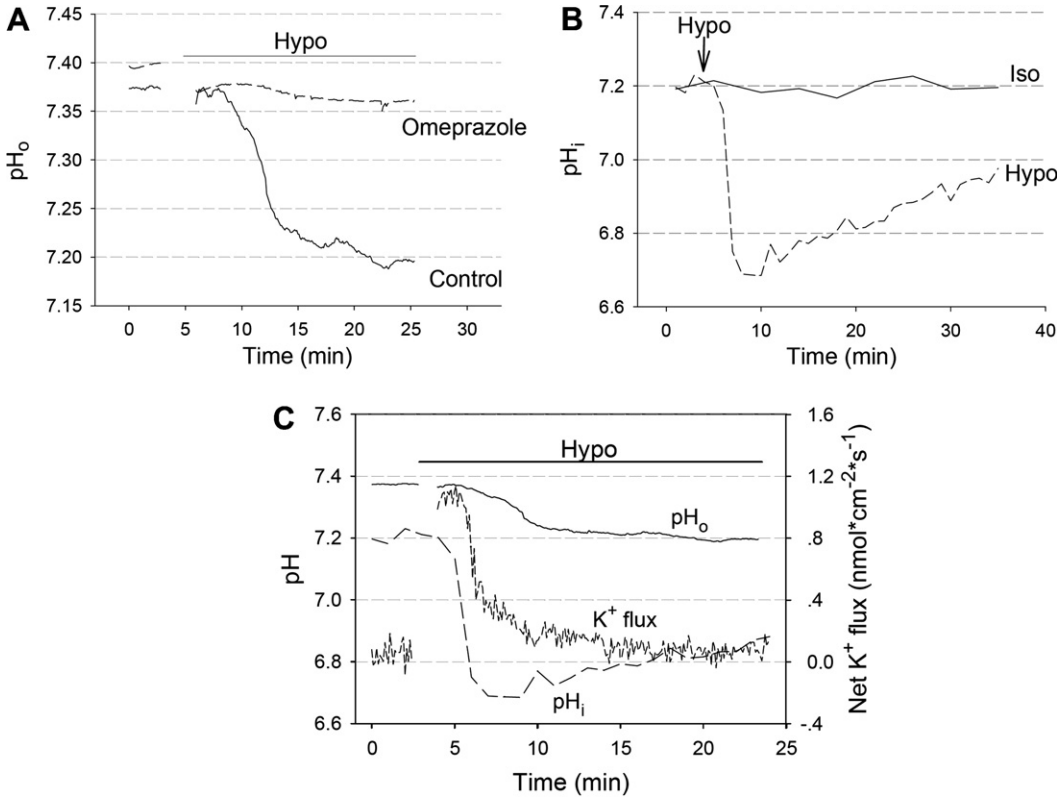

Fig. 5. Changes of extracellular pH (pH_o) and intracellular pH (pH_i) induced by hypotonic stimulation. (A) The typical time-course of extracellular pH changes in response to hypotonic stimulation (Control) and the inhibitory effect of 20 μM omeprazole on the hypotonicity-induced changes. The extracellular pH at the position of 1–2 μm away from the cell membrane was detected using the non-invasive micro-test technique. The pH measured 500 μm above cells was taken as the background recording (Blank). (B) The typical time-course of intracellular pH changes induced by hypotonic stimulation, detected using the pH sensitive fluorescent dye BCECF. (C) Temporal relationships between pH_o, pH_i and K^+ efflux.

Compared with that at pH 7.4, the hypotonicity-induced Cl^- efflux was activated earlier, and the peak value was slightly smaller when the bath pH was changed to 6.5 from 7.4 (Fig. 7A and B). The hypotonicity-activated Cl^- current was slightly increased at pH 6.5 (Fig. 7C and D).

3.9. Hypotonicity-induced RVD and effects of channels blockers, extracellular pH and the proton pump inhibitor omeprazole on the RVD

The cell volumes remained relatively constant under isotonic condition. When exposed to the 47% hypotonic bath solution, the cell volume was increased by 56.98 ± 4.45% in 3–5 min and then recovered gradually by a RVD process. The cell volume was recovered by 67.74 ± 11.10% ($n = 19$ cells in 5 independent experiments, $P < 0.01$) in 25 min when the hypotonic bath solution was kept at pH 7.4 (Control). The hypotonicity-induced RVD process was significantly inhibited by 100 μM clotrimazole and 10 μM tamoxifen, respectively ($P < 0.01$) (Fig. 8A). The hypotonicity-induced RVD process was also significantly inhibited by the decrease of pH from 7.4 to 6.5, and was facilitated by the treatment with 20 μM omeprazole ($P < 0.01$) (Fig. 8B).

4. Discussion

In this study, we first demonstrated that the hypotonicity-induced efflux of K^+ was different from that of Cl^- in activation and time course using the non-invasive micro-test technique. The activation of K^+ efflux was faster and only lasted for a relatively short period, compared with the Cl^- efflux. Furthermore, the activation and time course of the hypotonicity-induced K^+ and Cl^- fluxes detected by the non-invasive micro-test technique were different from the hypotonicity-activated K^+ and Cl^- currents recorded by the patch clamp technique. The activation of both currents was quick and sustained. Why the dynamics of hypotonicity-induced K^+ and Cl^- fluxes are different from that of hypotonicity-activated K^+ and Cl^- currents? There may be two possibilities. First, the regulation mechanism is intact in non-invasive ion flux recordings, but might have been impaired in patch-clamp current recordings. For example, the intracellular pH or the pH on cell surface is nearly physiologically regulated in non-invasive ion flux recordings, but the intracellular pH is almost fixed by the pipette solution in whole cell current recordings (discussed in more detail later). The difference in the ability to regulate ionic transport or to modulate ion channel activities may result in the difference in activation and time course between ion fluxes and currents. Second, the underlying mechanisms responsible for the ion fluxes may be different from those for the currents. The ion fluxes may be carried by ion channels and/or carriers, but the currents are mainly carried by ion channels. However, our results did not support this hypothesis. Our experiments demonstrate that both the fluxes and currents can be inhibited by channel blockers, indicating that both the ion effluxes and currents were mainly carried by ion channels.

Our data obtained with the non-invasive micro-test technique showed that the activation of the hypotonicity-induced K^+ efflux was ahead of that of hypotonicity-induced Cl^- and H^+ effluxes. Could the delayed transport of Cl^- and H^+ be due to slower kinetics of the resins compared to the K resin? In this study, the temporal characteristics of different ion-selective electrodes were similar, and the response time for the K^+, Cl^- or H^+ probe was less than 1 s during a step change in bath K^+, Cl^- or H^+. However, the activation

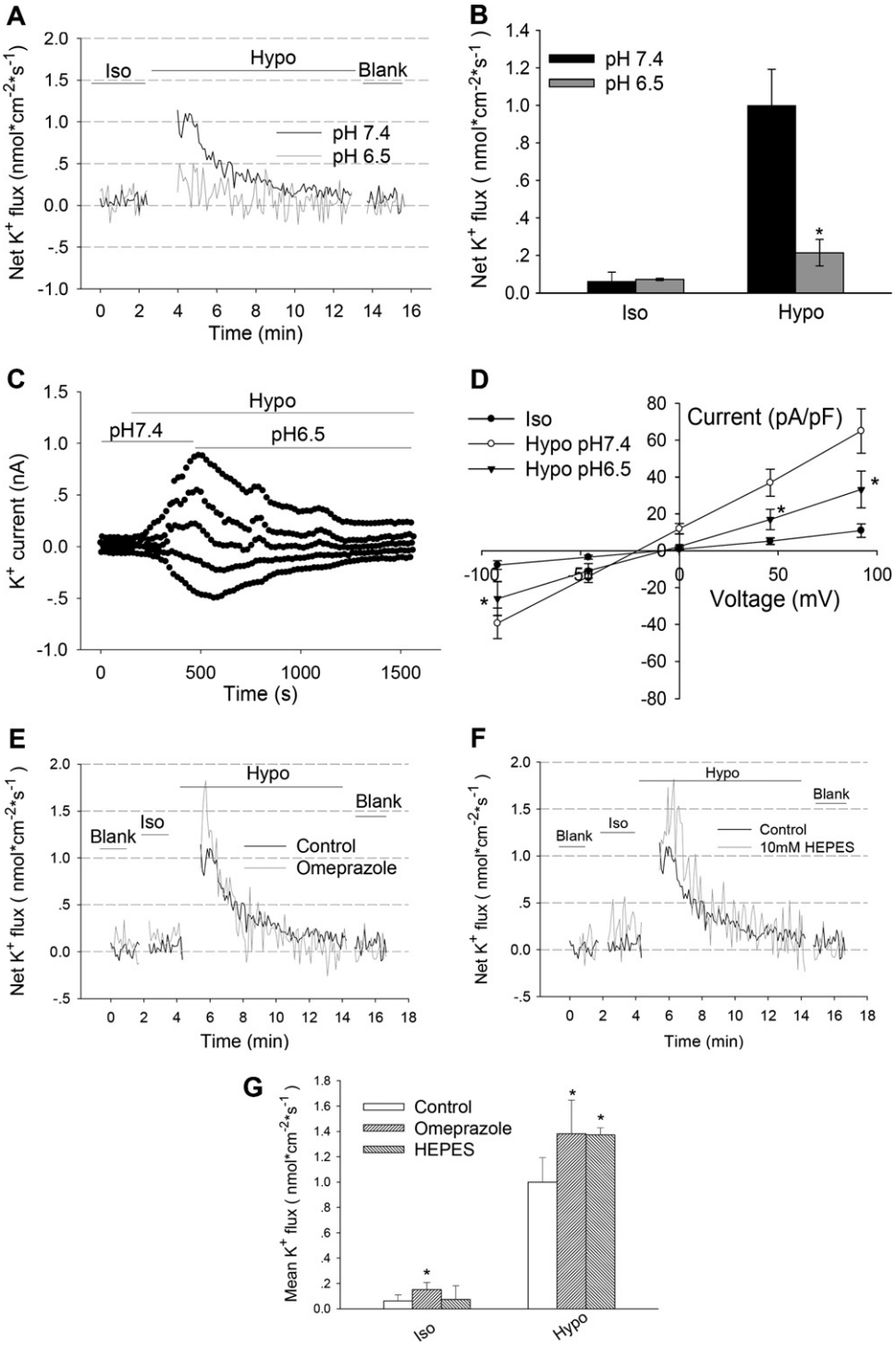

Fig. 6. Effects of extracellular pH on K^+ transport across the cell membrane. (A) Typical time-courses of K^+ efflux induced by 47% extracellular hypotonic stimulation at pH 7.4 and 6.5. K^+ efflux was detected by the non-invasive micro-test technique. Iso, isotonic bath solution. Hypo, 47% hypotonic solution. Blank, ion flux measured at the position of 500 μm away from cells. (B) Mean values of K^+ efflux induced by 47% extracellular hypotonic stimulation at pH 7.4 and 6.5 (n = 11 cells at pH 7.4, n = 6 cells at pH 6.5, mean ± S.E.M., $^*P < 0.05$, t-test). (C) The typical time-course of the K^+ current activated by 47% hypotonic bath solution at pH 7.4 and 6.5. The K^+ current was recorded using the patch clamp technique, with the potential held at 0 mV and stepped repeatedly to 0, ±46 and ±92 mV. (D) I–V relation ships of the K^+ current activated by 47% hypotonic bath solution at pH 7.4 and 6.5 (n = 6 cells, mean ± S.E.M., $^*P < 0.05$, Paired t-test, compared with pH 7.4). (E) The time-courses of K^+ efflux activated by 47% hypotonic stimulation and the effect of the proton pump inhibitor omeprazole (20 μM) on the efflux. (F) The time-course of K^+ efflux activated by 47% hypotonic stimulation and the effect of increase of pH buffer ability on the efflux by elevating HEPES concentration from 1 mM (control) to 10 mM (HEPES). (G) Mean K^+ effluxes under different conditions (n = 10–12 cells for different groups, mean ± S.E.M., $^*P < 0.05$ compared with Control, t-test).

of hypotonicity-induced Cl^- and H^+ effluxes was at least 3 min late compared with that of the K^+ efflux. The differences in activation of transport of K^+, Cl^- and H^+ could not be due to the small variation in response time of different electrodes.

Our data indicate that hypotonicity-induced K^+ efflux is transient, while Cl^- efflux is sustained. The phenomenon is different from the widely accepted concept that K^+ and Cl^- transport is tightly coupled in the process of RVD to retain charge

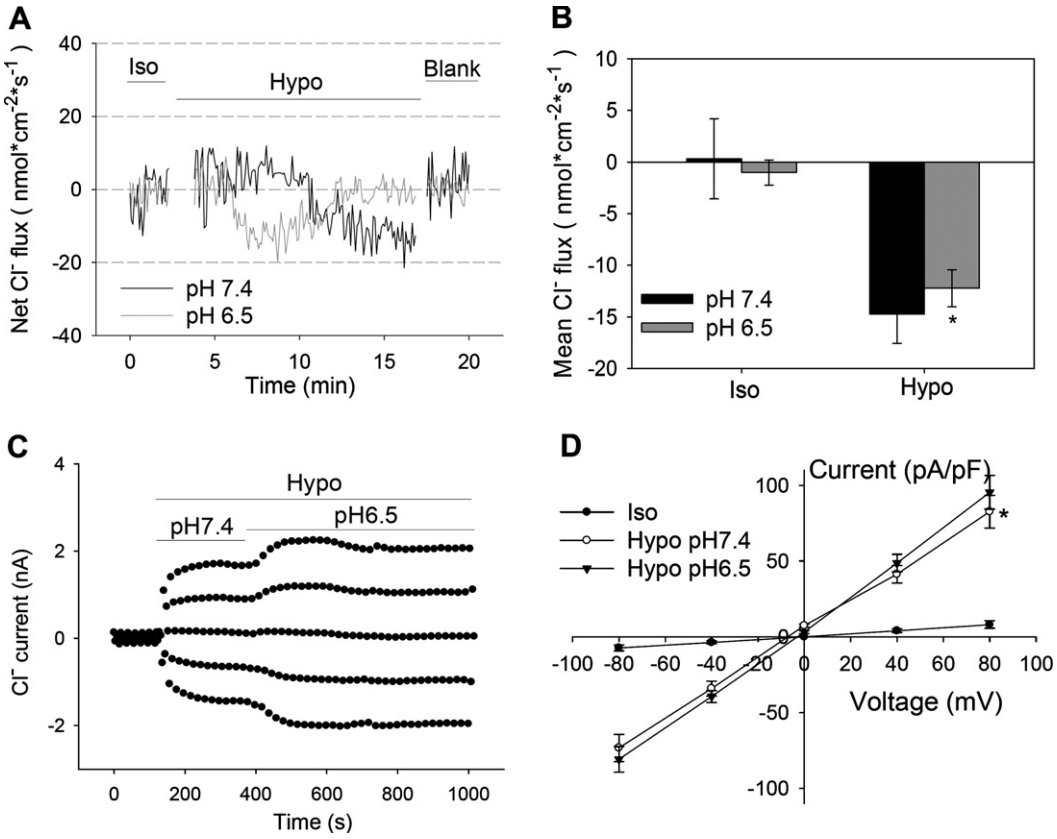

Fig. 7. Effects of extracellular pH on hypotonicity-induced Cl^- efflux and current. (A) Typical time-courses of Cl^- efflux activated by 47% hypotonic stimulation at pH 7.4 and 6.5, detected by the non-invasive micro-test technique. (B) Mean peak Cl^- efflux recorded at pH 7.4 and 6.5 (n = 12 cells at pH 7.4, n = 6 cells at pH 6.5, mean ± S.E.M. $^*P < 0.05$, t-test, compared with pH 7.4). (C) The typical time-course of the Cl^- currents activated by 47% hypotonic solution and effects of extracellular pH on the currents. The Cl^- current was detected by the patch-clamp technique with the potential held at 0 mV and stepped repeatedly to 0, ±40 and ±80 mV. (D) I–V relationships of Cl^- currents recorded under different conditions (n = 6 cells, mean ± S.E.M., $^*P < 0.05$, Paired t-test, compared with pH 7.4).

balance [31,32]. How can Cl^- transport remain relatively high when K^+ efflux has significantly declined? In this study, H^+ efflux in the process of hypotonicity-induced RVD was recorded for the first time with the non-invasive micro-test technique and results showed that the H^+ efflux was sustained. H^+ efflux may work as one of the substitutions of K^+ efflux to balance the potential changes induced by Cl^- efflux. It was reported that a transient Ca^{2+} influx or a transient increase in intracellular free Ca^{2+} was activated by hypotonic challenges with the time course similar to that of the hypotonicity-activated early K^+ efflux [33,34]. Ca^{2+} may be the counter ion for charge balance maintaining in the face of early K^+ transport activation.

Our data showed that hypotonic stimulation activated an H^+ efflux. The H^+ efflux was inhibited by the proton pump (H^+-K^+-ATPase) inhibitor omeprazole, suggesting that the H^+ efflux is mainly mediated by H^+-K^+-ATPase. The hypotonicity-induced H^+ efflux was Ca^{2+}-dependent. Depletion of extracellular Ca^{2+} abolished nearly completely the H^+ efflux. Further analysis indicates that omeprazole can only inhibited about 60% of the hypotonicity-induced H^+ efflux. This result suggests that besides

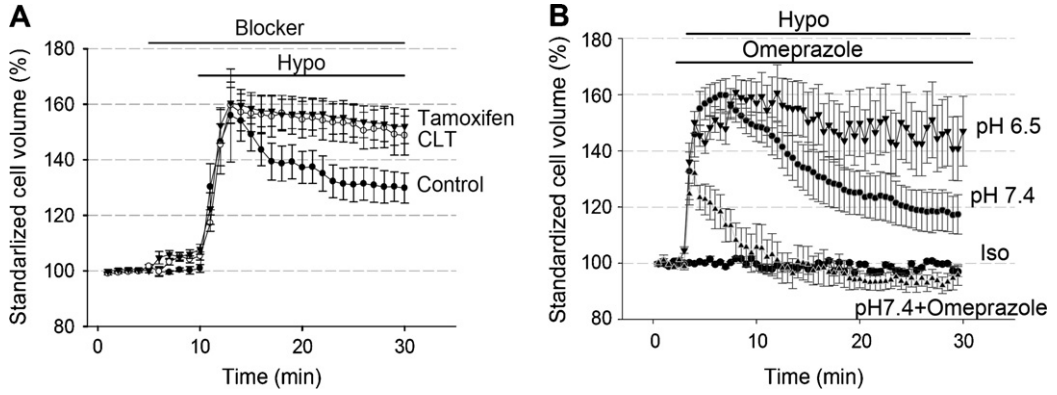

Fig. 8. Hypotonicity-induced RVD and the effects of channels blockers, extracellular pH and the proton pump inhibitor omeprazole on the RVD (n = 11–19, mean ± S.E.M.). (A) Cell volume changes in the 47% hypotonic bath solution (Control) and in 47% hypotonic bath solution containing 100 μM clotrimazole (CLT) or 10 μM tamoxifen were showed. (B) Cell volume changes in the isotonic bath solution at pH 7.4 (Iso), in the 47% hypotonic bath solution at pH 7.4 (pH 7.4), in the 47% hypotonic bath solution at pH 6.5 (pH 6.5) and in the 47% hypotonic bath solution containing 20 μM omeprazole at pH 7.4 (pH 7.4 + Omeprazole) were showed.

H^+-K^+-ATPase, other Ca^{2+}-dependent H^+ transport mechanisms may also be associated with the H^+ efflux.

We found that both intracellular pH and extracellular pH were decreased during the hypotonic challenge. Furthermore, the decrease of intracellular pH was ahead of activation of H^+ efflux and decline of extracellular pH, and the following recover process of intracellular pH was paralleled with the decrease of extracellular pH. These results imply that the decrease of intracellular pH may be the trigger factor for activation of H^+ efflux and extracellular pH decrease. We also found that the onset of hypotonicity-induced decline of extracellular pH was coincident with activation of H^+ efflux, and that both hypotonicity-induced H^+ efflux and extracellular pH decrease were inhibited by the proton pump inhibitor omeprazole. These data indicate that the decrease of extracellular pH is caused mainly by the H^+ efflux.

In present study, it was demonstrated that hypotonicity-induced K^+ efflux was transient. The onset of K^+ efflux decline was coincident with activation of H^+ efflux. These results imply that extracellular acidification may be responsible for the decline of hypotonicity-induced K^+ efflux by inhibiting volume-activated K^+ channels. This hypothesis is verified by our further experiments. Our results showed that decrease of extracellular pH had an inhibitory effect on the hypotonicity-activated K^+ current recorded by the patch clamp technique and K^+ efflux detected by the non-invasive micro-test technique. If extracellular and intracellular pH is fixed, as in the whole cell patch clamp experiments, the hypotonicity-activated K^+ flow should be sustained. In this study, it was proved that increasing pH buffer ability by elevating the concentration of the pH buffer HEPES or blocking H^+ secretion with omeprazole enhanced the hypotonicity-induced K^+ efflux.

However, omeprazole only enhanced the peak, not steady state value, of K^+ transport although omeprazole completely abolished extracellular acidification. It was reported that intracellular acidification inhibited the activity of the IK1 channels [19]. We demonstrated in this study that intracellular pH was decreased by the hypotonic challenge. It is possible that the decrease of intracellular pH is one of the mechanisms underlying inhibition of steady state K^+ transport.

We have also reported that Ca^{2+}-activated K^+ channels were the main component of volume activated K^+ channels in CNE-2Z cells [11]. It has also been reported that the potassium channel protein IK1 undergoes transient volume-sensitive translocalization under hypotonic stimulation [13]. The volume-activated K^+ efflux in present study presents similar time course with IK1 translocalization. The decrease of extracellular pH might be responsible for the alteration of IK1 spatial localization in the plasma membrane, resulting in a decrease of channel numbers in plasma membrane and thus the decline of K^+ efflux.

It was demonstrated in this study that moderate decrease of extracellular pH did not inhibit, but enhanced volume-activated Cl^- currents. The purinergic receptor pathways have been proposed to be involved in activation of Cl^- currents under hypotonic conditions [31], and extracellular pH decrease may facilitate ATP and its Mg^{2+} and/or H^+ salts exit cells in anionic forms [35]. Our previous studies have shown that ClC-3 chloride channel is the component or regulator of the volume activated Cl^- current in CNE-2Z cells [1–3], and its up-regulation of expression in CNE-2Z cells compared with normal human nasopharyngeal epithelial cells [36]. Extracellular acidosis is a hallmark of solid tumors as a result of high glycolytic flux and poor vascular perfusion [37]. The low extracellular pH may promote malignant behavior of tumor cells through activation of volume-activated Cl^- channels. As a result, methods to overcome this acidosis condition may be an ideal therapeutic strategy in the volume-activated Cl^- channel up regulated tumor cells.

As showed above, we demonstrated in this study that K^+ and Cl^- transport in hypotonicity-induced RVD process was uncoupled; the decrease of extracellular pH induced by H^+ efflux accounted for the inactivation of volume-activated K^+ channels. The effects of extracellular pH on RVD were also proved in our experiments. The hypotonicity-induced RVD was inhibited by extracellular acidification, coincident with the sensitivity of volume-activated K^+ channels to extracellular pH. Blocking H^+ secretion with the proton pump inhibitor omeprazole facilitated the RVD process. Numerous proteins that play crucial roles in intercellular communication, signal transduction, cytoskeletal dynamics and vesicle trafficking have been reported to be highly sensitive to the concentration of H^+, and pH is suggestive of a role in signaling [38]. H^+ efflux and extracellular pH may function as the regulators of ion channels and may further function in regulation of tumor cell proliferation, migration and apoptosis.

As a summary, opposite to the widely accepted concept that K^+ and Cl^- transport is tightly coupled in the process of RVD, we prove for the first time in this study that the K^+ and Cl^- transport in the process of hypotonicity-induced RVD are uncoupled, with the transient K^+ efflux activated earlier and sustained Cl^- efflux activated later. The sensitivity of K^+ and Cl^- channels to extracellular pH was different. The decrease of extracellular pH caused by the hypotonicity-induced H^+ efflux is responsible for the inactivation of volume-activated K^+ channels in the late stage of RVD. H^+ may function as a key regulator of volume-activated ion channels which play important roles in regulation of cell function, and may be a therapeutic target for human nasopharyngeal carcinoma.

Conflicts of interest

No potential conflicts of interest were disclosed.

Acknowledgments

We thank Professor Ole H. Petersen (Cardiff School of Biosciences, Cardiff University, UK) for his great comments on this manuscript. This work was supported by the National Natural Science Foundation of China (Nos. 30771106, 30870567, 30871267, and U0932004/L02) and by Jinan University (No. 216113113).

References

[1] Chen L, Wang L, Zhu L, Nie S, Zhang J, Zhong P, et al. Cell cycle-dependent expression of volume-activated chloride currents in nasopharyngeal carcinoma cells. Am J Physiol Cell Physiol 2002;283:C1313–23.
[2] Chen LX, Zhu LY, Jacob TJ, Wang LW. Roles of volume-activated Cl^- currents and regulatory volume decrease in the cell cycle and proliferation in nasopharyngeal carcinoma cells. Cell Prolif 2007;40:253–67.
[3] Mao J, Chen L, Xu B, Wang L, Li H, Guo J, et al. Suppression of ClC-3 channel expression reduces migration of nasopharyngeal carcinoma cells. Biochem Pharmacol 2008;75:1706–16.
[4] Yang L, Ye D, Ye W, Jiao C, Zhu L, Mao J, et al. ClC-3 is a main component of background chloride channels activated under isotonic conditions by autocrine ATP in nasopharyngeal carcinoma cells. J Cell Physiol 2011;226:2516–26.
[5] Lang F, Foller M, Lang K, Lang P, Ritter M, Vereninov A, et al. Cell volume regulatory ion channels in cell proliferation and cell death. Methods Enzymol 2007;428:209–25.
[6] Okada Y, Shimizu T, Maeno E, Tanabe S, Wang X, Takahashi N. Volume-sensitive chloride channels involved in apoptotic volume decrease and cell death. J Membr Biol 2006;209:21–9.
[7] Jakab M, Schmidt S, Grundbichler M, Paulmichl M, Hermann A, Weiger T, et al. Hypotonicity and ethanol modulate BK channel activity and chloride currents in GH4/C1 pituitary tumour cells. Acta Physiol (Oxf) 2006;187:51–9.
[8] Bortner CD, Cidlowski JA. Cell shrinkage and monovalent cation fluxes: role in apoptosis. Arch Biochem Biophys 2007;462:176–88.
[9] Lambert IH, Klausen TK, Bergdahl A, Hougaard C, Hoffmann EK. ROS activate KCl cotransport in nonadherent Ehrlich ascites cells but K+ and Cl^- channels in adherent Ehrlich Lettre and NIH3T3 cells. Am J Physiol Cell Physiol 2009; 297:C198–206.

[10] Okada Y, Sato K, Numata T. Pathophysiology and puzzles of the volume-sensitive outwardly rectifying anion channel. J Physiol 2009;587:2141–9.
[11] He ST, Zhu LY, Yang LJ, He SC, Mao JW, Wang LW, et al. $Ca^{(2+)}$-dependent potassium channels play important roles in regulatory volume decrease in human nasopharyngeal carcinoma cells. Sheng Li Xue Bao 2009;61:485–92.
[12] Wang J, Morishima S, Okada Y. IK channels are involved in the regulatory volume decrease in human epithelial cells. Am J Physiol Cell Physiol 2003;284:C77–84.
[13] Barfod ET, Moore AL, Roe MW, Lidofsky SD. Ca^{2+}-activated IK1 channels associate with lipid rafts upon cell swelling and mediate volume recovery. J Biol Chem 2007;282:8984–93.
[14] Lee EL, Hasegawa Y, Shimizu T, Okada Y. IK1 channel activity contributes to cisplatin sensitivity of human epidermoid cancer cells. Am J Physiol Cell Physiol 2008;294:C1398–406.
[15] Shumilina E, Lam RS, Wolbing F, Matzner N, Zemtsova IM, Sobiesiak M, et al. Blunted IgE-mediated activation of mast cells in mice lacking the Ca^{2+}-activated K^+ channel KCa3.1. J Immunol 2008;180:8040–7.
[16] Lo C, Ferrier J, Tenenbaum HC, McCulloch CA. Regulation of cell volume and intracellular pH in hyposmotically swollen rat osteosarcoma cells. Biochem Cell Biol 1995;73:535–44.
[17] Smets I, Ameloot M, Steels P, Van Driessche W. Loss of cell volume regulation during metabolic inhibition in renal epithelial cells (A6): role of intracellular pH. Am J Physiol Cell Physiol 2002;283:C535–44.
[18] Hougaard C, Jorgensen F, Hoffmann EK. Modulation of the volume-sensitive K^+ current in Ehrlich ascites tumour cells by pH. Pflugers Arch 2001;442:622–33.
[19] Pedersen KA, Jorgensen NK, Jensen BS, Olesen SP. Inhibition of the human intermediate-conductance, Ca^{2+}-activated K^+ channel by intracellular acidification. Pflugers Arch 2000;440:153–6.
[20] Matsuda JJ, Filali MS, Volk KA, Collins MM, Moreland JG, Lamb FS. Overexpression of CLC-3 in HEK293T cells yields novel currents that are pH dependent. Am J Physiol Cell Physiol 2008;294:C251–62.
[21] Matsuda JJ, Filali MS, Collins MM, Volk KA, Lamb FS. The ClC-3 Cl^-/H^+ antiporter becomes uncoupled at low extracellular pH. J Biol Chem 2010;285:2569–79.
[22] Gilliham M, Sullivan W, Tester M, Tyerman SD. Simultaneous flux and current measurement from single plant protoplasts reveals a strong link between K^+ fluxes and current, but no link between Ca^{2+} fluxes and current. Plant J 2006;46:134–44.
[23] Smith PJ, Trimarchi J. Noninvasive measurement of hydrogen and potassium ion flux from single cells and epithelial structures. Am J Physiol Cell Physiol 2001;280:C1–1.
[24] Sun J, Chen S, Dai S, Wang R, Li N, Shen X, et al. NaCl-induced alternations of cellular and tissue ion fluxes in roots of salt-resistant and salt-sensitive poplar species. Plant Physiol 2009;149:1141–53.
[25] Messerli MA, Collis LP, Smith PJ. Ion trapping with fast-response ion-selective microelectrodes enhances detection of extracellular ion channel gradients. Biophys J 2009;96:1597–605.
[26] Garber SS, Messerli MA, Hubert M, Lewis R, Hammar K, Indyk E, et al. Monitoring Cl^- movement in single cells exposed to hypotonic solution. J Membr Biol 2005;203:101–10.
[27] Shirihai O, Smith P, Hammar K, Dagan D. Microglia generate external proton and potassium ion gradients utilizing a member of the H/K ATPase family. Glia 1998;23:339–48.
[28] Chen LX, Wang LW. Volume-activated chloride current in pigmented ciliary epithelial cells. Sheng Li Xue Bao 2000;52:421–6.
[29] Schwiening CJ, Boron WF. Regulation of intracellular pH in pyramidal neurones from the rat hippocampus by $Na^{(+)}$-dependent $Cl^{(-)}$-HCO^{3-} exchange. J Physiol 1994;475:59–67.
[30] Mao JW, Wang LW, Jacob T, Sun XR, Li H, Zhu LY, et al. Involvement of regulatory volume decrease in the migration of nasopharyngeal carcinoma cells. Cell Res 2005;15:371–8.
[31] Okada Y, Maeno E, Shimizu T, Dezaki K, Wang J, Morishima S. Receptor-mediated control of regulatory volume decrease (RVD) and apoptotic volume decrease (AVD). J Physiol 2001;532:3–16.
[32] Hoffmann EK, Lambert IH, Pedersen SF. Physiology of cell volume regulation in vertebrates. Physiol Rev 2009;89:193–277.
[33] Becker D, Blase C, Bereiter-Hahn J, Jendrach M. TRPV4 exhibits a functional role in cell-volume regulation. J Cell Sci 2005;118:2435–40.
[34] Kerrigan MJ, Hall AC. Control of chondrocyte regulatory volume decrease (RVD) by $[Ca^{2+}]i$ and cell shape. Osteoarthritis Cartilage 2008;16:312–22.
[35] Sabirov RZ, Okada Y. ATP release via anion channels. Purinergic Signal 2005;1:311–28.
[36] Zhu L, Yang H, Zuo W, Yang L, Zhang H, Ye W, et al. Differential expression and roles of volume-activated chloride channels in control of growth of normal and cancerous nasopharyngeal epithelial cells. Biochem Pharmacol 2012;83:324–34.
[37] Wojtkowiak JW, Verduzco D, Schramm KJ, Gillies RJ. Drug resistance and cellular adaptation to tumor acidic pH microenvironment. Molecular pharmaceutics 2011;8:2032–8.
[38] Casey JR, Grinstein S, Orlowski J. Sensors and regulators of intracellular pH. Nat Rev Mol Cell Biol 2010;11:50–61.